Paper presented at ICDS-12
Amsterdam, August 31 - September 3, 1982

Physica 116B (1983) 224-229
North-Holland Publishing Company

THE NEGATIVELY CHARGED VACANCY IN SILICON: HYPERFINE INTERACTIONS FROM ENDOR MEASUREMENTS

M. SPRENGER, S.H. MULLER and C.A.J. AMMERLAAN

Natuurkundig Laboratorium, Universiteit van Amsterdam
Valckenierstraat 65, 1018 XE Amsterdam, The Netherlands

The negatively charged lattice vacancy V^- was produced in p-type aluminum doped silicon by 1.5 MeV electron irradiation at temperatures below 20 K. The Si-G2 EPR spectrum, which is associated with the negative charge state of the lattice vacancy, was investigated by electron nuclear double resonance. Hyperfine interactions between the unpaired defect electron and ^{29}Si nuclei on various lattice sites with respect to the vacancy were determined in order to obtain detailed information about the electron wave function. By symmetry, there are four classes of lattice sites around the vacancy, therefore there are four distinguishable classes of hyperfine interaction tensors. Values for the contact term of the hyperfine interactions are reported for 27 shells containing 73 atoms. The one-electron LCAO scheme to describe the electron wave function is discussed. Also, the extension and shape of the defect electron distribution is discussed in an empirical manner.

1. INTRODUCTION

Among all the known defects in silicon the vacancy has probably received the greatest interest over the last 20 years, as well in experimental as in theoretical physical research. The vacancy is an important defect as it is in fact one of the two primary defects in the irradiation damage process. Moreover it is one of the simplest defect structures in the diamond lattice to perform calculations on.

Back in 1965 Watkins identified the EPR spectra Si-G1 and Si-G2 with the vacancy in its positive and negative charge state, respectively [1]. More recently insight was gained in the level structure of the various charge states of the vacancy by EPR and DLTS measurements [2,3,4]. Especially the negative-U character of the charge states V^{++}, V^+ and V^0 gained much attention. Also in recent years important progress was made in the development of new theoretical techniques such as the selfconsistent pseudopotential Green's function method [5,6].

In this paper we report electron nuclear double resonance (ENDOR) measurements on the EPR spectrum Si-G2, associated with the vacancy in its negative charge state (V^-). The ENDOR technique can be used to obtain very accurate values for the hyperfine interaction parameters with a large number of ^{29}Si nuclei on lattice sites surrounding the vacancy. As these hyperfine interactions reflect the local density distribution of the unpaired defect electron, information on its wave function is obtained.

In section 2 a short description of our experiments is given, in section 3 we present the isotropic parts of the hyperfine interactions for 27 shells of lattice sites, containing 73 atoms. Section 4 is attributed to a discussion on the implications of our results for the LCAO scheme commonly used for description of the vacancy. Also in section 4 a discussion is given on the possible extension and shape of the electron wave function.

2. EXPERIMENTAL

As vacancies in silicon are highly mobile at room temperature, the sample has to be kept at low temperatures during irradiation and measurements.

We produced vacancies by irradiation of 0.9 Ωcm aluminum doped float-zone silicon, containing 2×10^{16} Al.cm^{-3}, with 1.5 MeV electrons at temperatures below 20 K to a fluence of 10^{17}

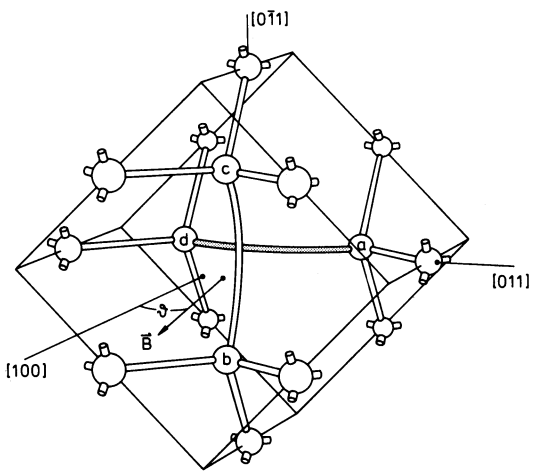

Fig.1. Model of the negatively charged vacancy in orientation ad. The magnetic field can be rotated in the (0$\bar{1}$1)-plane.

electrons.cm^{-2}. After the irradiation V^- was the stable charge state of the vacancy in a concentration of about 10^{16} .cm^{-3}, as well before as after a 30K anneal.

EPR and ENDOR measurements were performed using a superheterodyne spectrometer operating at 23 GHz. The magnetic field could be rotated in the $(0\bar{1}1)$ plane of the silicon sample. Best results for ENDOR were obtained at a temperature of 18 K, using a double phase sensitive detection at the frequencies of 83 Hz for the EPR magnetic field modulation and 3.3 Hz for the square wave modulation of the RF-field for ENDOR. Except for the cryostat most of the experimental set-up was equal to that used by de Wit [7] and Sieverts [8].

3. OUTLINE OF EXPERIMENTAL RESULTS

The EPR and ENDOR spectra of the vacancy are accurately described by the spin Hamiltonian:

$$\mathscr{H} = \mu_B \vec{B}.\overleftrightarrow{g}.\vec{S} + \sum_i (\vec{S}.\overleftrightarrow{A}_i.\vec{I}_i - g_N \mu_N \vec{B}.\vec{I}_i) \qquad (1)$$

The first term is the Zeeman interaction between the unpaired defect electron $\vec{S}$ (S=1/2) and the magnetic field $\vec{B}$. The summation runs over lattice sites: $\overleftrightarrow{A}_i$ is the hyperfine tensor of the interaction of the defect electron with the nuclear spin $\vec{I}$ (I=1/2, 4.7% abundant) of a ^{29}Si nucleus at site i . The second term in the summation is the nuclear Zeeman term. The EPR transitions are defined by $\Delta m_S=\pm 1$, $\Delta m_I=0$, the ENDOR transitions by $\Delta m_I=\pm 1$, $\Delta m_S=0$.

Fig. 1 shows a model of the vacancy in one of its six possible orientations. This orientation, denoted by ad, is our standard orientation to which all orientation-dependent information refers. The symmetry of the g-tensor is 2mm, having 3 independent parameters. The symmetry of the A-tensor, being the symmetry of the system (vacancy plus ^{29}Si atom at site i) depends on the location of the magnetic nucleus with respect to the vacancy. It is 2mm for sites on the twofold axis of the vacancy (tensors of twofold-axis class T), m for sites in one of both mirrorplanes (mirrorplane class tensors Mad or Mbc) and 1 for sites in none of the mirrorplanes (general class tensors G). Properties of these four tensor classes are given in table I.

Table I. Properties of the different types of hyperfine tensors and associated shells for the vacancy V^-. N_{at}= number of atoms per shell. N_{el}= number of independent tensor elements. Atom positions refer to orientation ad.

Class	Symmetry	N_{el}	N_{at}	Atom positions
T	2mm	3	1	[100]-axis
Mad	m	4	2	$(0\bar{1}1)$-plane
Mbc	m	4	2	(011)-plane
G	1	6	4	others

The nuclear Zeeman interaction is isotropic and described by 1 parameter.

Parameters were determined by computer diagonalisation of the 4 x 4 Hamiltonian and fitting in a least squares program. From EPR data first the g-tensor was fitted, giving g_1=2.0151, g_2=2.0028, and g_3=2.0042, in close agreement with Watkins' values [1]. The nuclear Zeeman interaction parameter was determined to be 8.4592 MHz.T^{-1}, also by computer fit of one specific hyperfine tensor of which the ENDOR transitions were measured for both m_S=+1/2 and m_S=-1/2 . In order to fit the hyperfine tensor elements, these electronic and nuclear g-values were kept constant. Only the high frequency ENDOR transitions were used. In all cases fits were achieved to within half of the linewidth at half height, mostly better. Linewidths ranged from 1.5 kHz for the smaller hyperfine interactions to 60 kHz for the largest, Mad1 at frequencies of 160 - 200 MHz. This tensor is the one that can be determined in EPR also, with much less accuracy [1].

Fig.2 shows an example of an ENDOR spectrum, clearly showing the symmetry around the nuclear Zeeman frequency ν_z, which is about 7 MHz for our values of the magnetic field. This spectrum shows the resolving power of ENDOR, however our signal to noise ratio was better in most cases than in this extremely compressed spectrum.

So far 27 hyperfine tensors have been unraveled. Values for the isotropic part of the hyperfine interactions a_i are listed in table II. These isotropic parts originate from the Fermi contact interaction:

$$a_i = 8/3\pi g \mu_B g_N \mu_N |\psi(\vec{r}_i)|^2 \qquad (2)$$

giving a relation with the probability density of the defect electron on the nuclear site i. Thus, the value $|\psi(\vec{r}_i)|^2$ can be calculated numerically from:

$$a_i(\text{MHz}) = 131.928 \times |\psi(\vec{r}_i)|^2 \ (\text{Å}^{-3}). \qquad (3)$$

Table II. Isotropic parts of the hyperfine interaction tensors a_i=1/3 Tr($\overleftrightarrow{A}_i$). Enumeration is in decreasing magnitude of a_i. Units are MHz.

Number	G	Mad	Mbc	T
1	13.359	355.845	2.106	0.666
2	7.963	50.203	1.998	
3	4.844	30.521	0.830	
4	2.705	13.468	0.203	
5	2.062	6.319		
6	2.020	3.077		
7	2.005	2.375		
8	1.752	1.520		
9	1.390	1.184		
10	1.381	1.072		
11		1.063		
12		0.813		

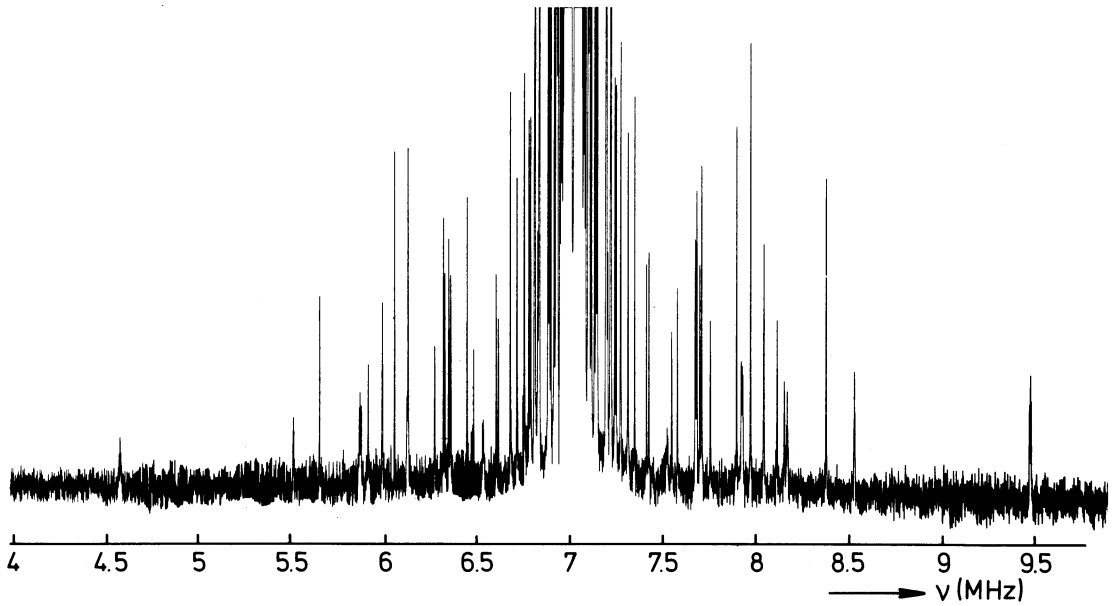

Fig.2. Endor spectrum for vacancy orientations ad and bc, with the magnetic field B=827.82 mT parallel to [100], demonstrating the symmetry around the nuclear Zeeman frequency, ν_z=7.0027 MHz.

As an illustration of the properties of the hyperfine tensors figures 3 to 6 show the angular dependence of the largest tensor of every class (Mad1, G1, Mbc1, T1). Plotted is the quantity $\nu-\nu_z$, with ν the ENDOR frequency, calculated with the fitted parameters and ν_z the nuclear Zeeman frequency. These values are, to first order, equal to $\frac{1}{2}\vec{b}.\overleftrightarrow{A}.\vec{b}$, with $\vec{b}$ a unit vector in the direction of the magnetic field, so that these plots give in fact the angular dependence of the hyperfine interactions. Tensors Mad1 and G1 clearly show nearly <111>-axial symmetry, whereas the others do not.

4. DISCUSSION

The first point to be discussed is the mere existence of contact hyperfine interactions with atoms in the plane of the atoms b and c for vacancy orientation ad.

In the one-electron LCAO molecular orbital model commonly used for description of the electronic structure of the vacancy [1,9], the unpaired electron of V^- has a b_1 type wave function. Considering only the dangling bonds of the four nearest neighbours a,b,c and d this LCAO wave function is a-d. Fig.7(a) shows the level scheme and wave functions of the vacancy in this LCAO model. However, an electron in the b_1 level has a wave function which is antisymmetric with respect to reflection in the plane of b and c. This requires a vanishing electron density $|\psi(\vec{r}_1)|^2$ on sites in this plane. As can be inferred from the existence of hyperfine tensors of classes Mbc and T with a≠0 this is clearly not the case, although they are small compared to the largest interactions of the classes G and Mad.

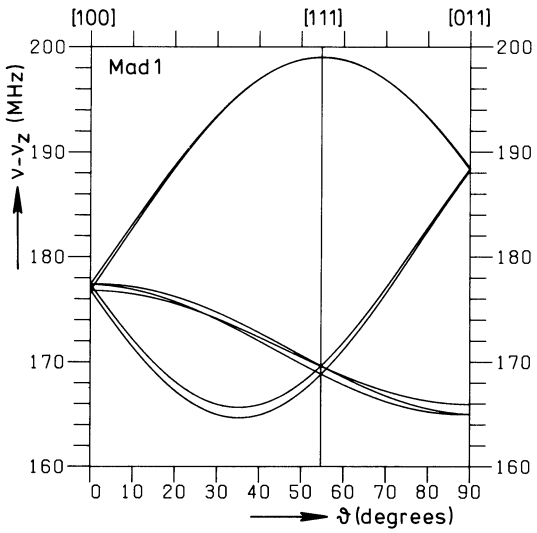

Fig.3. Angular dependence of the largest hyperfine tensor of the class Mad. This interaction has nearly <111>-axial symmetry.

To allow for non-zero contact hyperfine interactions on all atom sites in the one electron model a wave function of symmetry type a_1 is required. This is the only symmetry type within the pointgroup 2mm in which s-type orbitals can exist on atoms in both mirrorplanes and on the twofold axis. In the usual energy level diagram, fig.7(a), the ground state is b_1. However, an alternative level ordering, as in fig.7(b) may be considered. In this case a larger shift of the b_1 level due to the trigonal distortion is assumed. This large effect of the trigonal distortion, compared to the effect of the preceding tetragonal distortion, is in fact corroborated by estimates of the corresponding Jahn-Teller energies [10]. The effect of the trigonal distortion is estimated to be about equal to that of the tetragonal distortion. As a consequence of the one-electron ground state of fig.7(b), the electron occupies the a_1 level corresponding to the molecular orbital a+d. To this state an admixture λ(b+c) of the other a_1 state can exist. The full wave function a+d+λ(b+c) then allows for an adequate description of the contact hyperfine terms. Assuming for the moment that tensor Mbc1 is associated with the shell of atoms b and c one estimates λ=0.07.

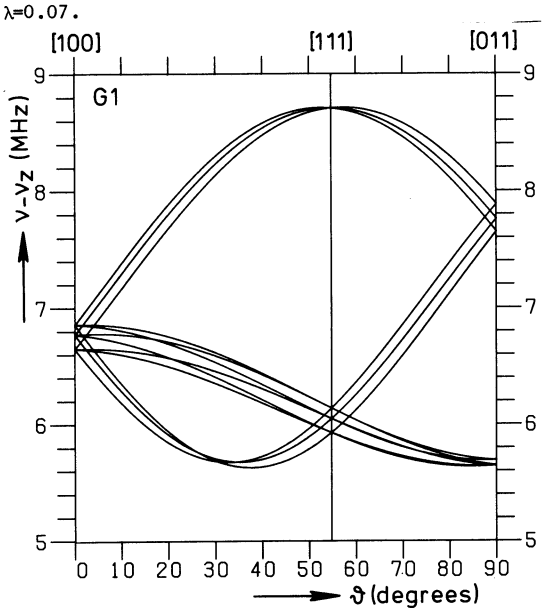

Fig.4. Angular dependence of the largest general class hyperfine tensor G1. This interaction has nearly <111>-axial symmetry.

An alternative explanation can be found by considering the effect of correlation, which goes beyond the one-electron description. The ground state of the 5-electron system V^- is given by the configuration $(a_1'\bar{a}_1'a_1''\bar{a}_1''b_1)$, where the bar denotes antiparallel spin. This corresponds to a $^2B_1$ state. The other configurations with the same symmetry are $(a_1'\bar{a}_1'b_1b_2\bar{b}_2)$, $(a_1''\bar{a}_1''b_1b_2\bar{b}_2)$ and $(a_1'\bar{a}_1''b_1b_2\bar{b}_2)$. By configuration interaction these excited states will mix in to the ground state. Of these only the third has a non-vanishing spin density at the mirrorplane bc. In this concept, the contact terms of the tensors of type Mbc are a measure of correlation effects. Experimental values in table II show a fairly small contact term for class Mbc compared to class Mad. Therefore the effect of correlation on the wave function is small. This can be an explanation for the success of the one-electron treatment.

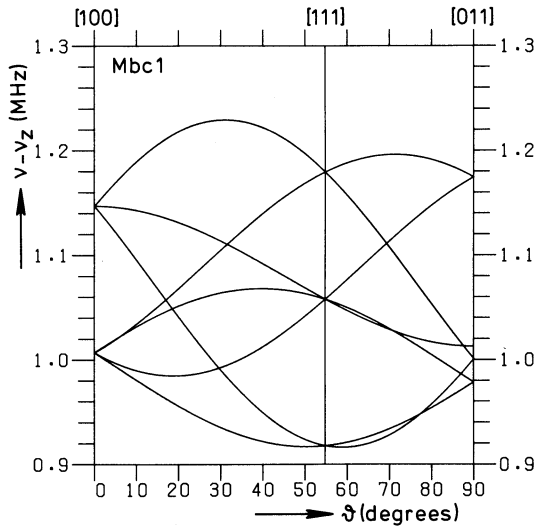

Fig.5. Angular dependence of the largest tensor of class Mbc.

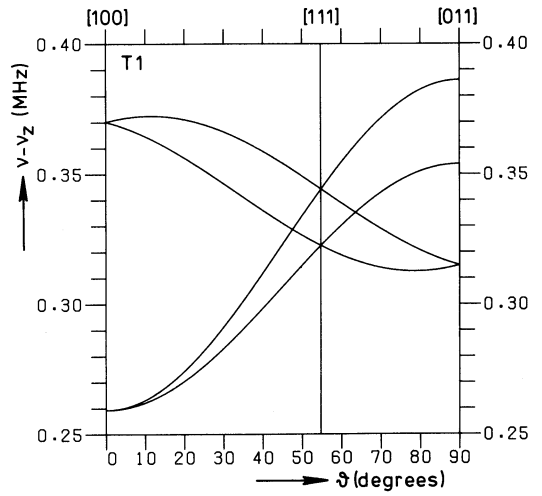

Fig.6. Angular dependence of the largest hyperfine tensor of class T.

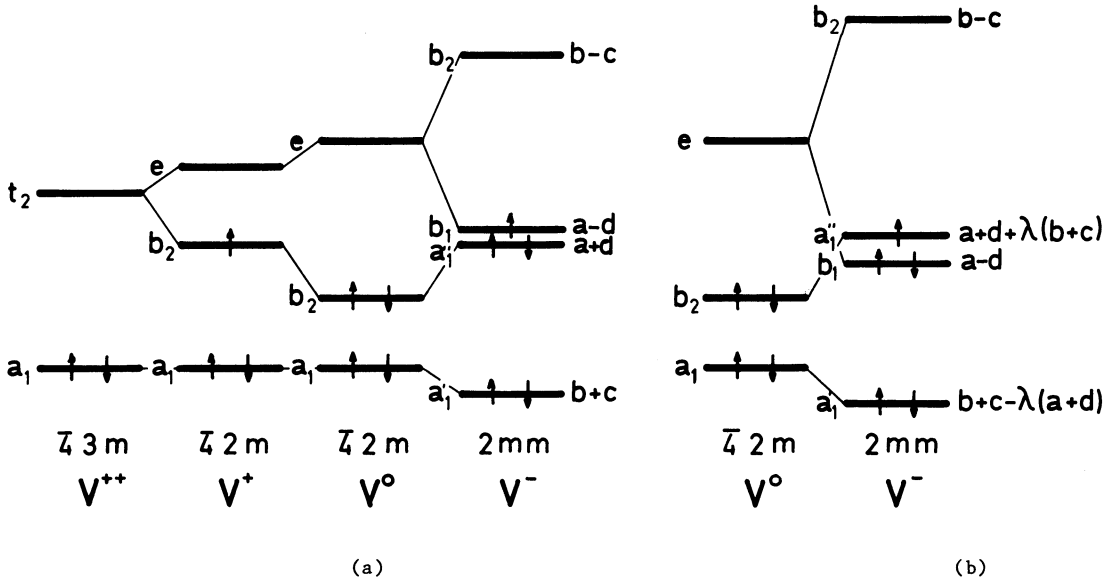

Fig.7. (a) LCAO level scheme of the vacancy in its various charge states from [9].
(b) as in (a), assuming that the trigonal distortion of V^- is so large, that the b_1 level lies under the a_1''-level.

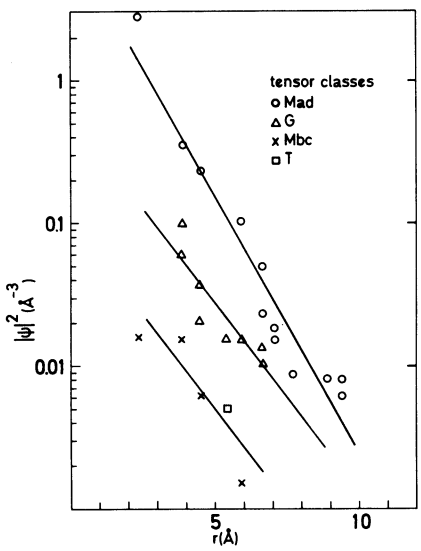

Fig.8. Hyperfine interactions of the negatively charged vacancy in silicon, converted to values for the wave function, plotted against distance from the vacancy. Full lines are approximations with exponential decrease.

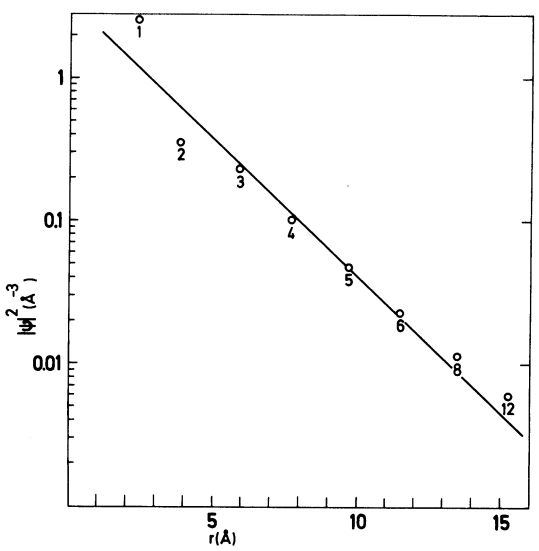

Fig.9. As fig.8, for distances of the atoms along a [011] chain.

Table III. Parameters of the function A^2e^{-2r/r_o}, fitted to the values of $|\psi(\vec{r})|^2$ of the vacancy and divacancy in silicon.

Defect	Type of shell	A^2 ($Å^{-3}$)	r_o (Å)
V^-	Mad	10	2.4
V^-	Mbc	0.1	3.0
V^-	G	0.6	3.2
V^-	Mad†	3.3	4.7
VV^-	M	2	3.0
VV^-	G	1.1	2.6
VV^+	M	7	1.9
VV^+	G	4.3	1.9

† assuming the atoms along the [011]-chain, see text.

A second point of discussion is the spatial extension of the electron wave function. An important objective of measuring hyperfine parameters by ENDOR is to bring about a complete assignment of hyperfine tensors to shells of lattice sites. Apart from the classification of tensors in classes, the experimental results give no further direct clues to the solution of this problem. Support has to be obtained from theoretical considerations, but at this moment sufficiently detailed results are not available. Nevertheless, some general picture of the wave function can be given. In fig.8 we plot the probability density $|\psi(\vec{r}_i)|^2$ as a function of distance r, assuming for the moment that the distribution of hyperfine tensors over lattice sites is such that the wave function decreases monotonously with the distance. An analysis in the same spirit was given for the divacancy by Sieverts, who also discussed the validity of this empirical treatment [11].

An important point which emerges from this picture is that the probability density in the plane of atoms a and d is much larger than outside this plane. The experimental data points are fitted with the purely empirical assumption of exponential decrease. The parameters A^2 and r_o of these fits are listed in table III, together with the parameters one obtains when fitting the data of the divacancy to this function [7,8,11]. It is important to notice that the "extent" r_o of the wave function of V^- is comparable to the case of VV^-, whereas the confinement of the wave function to the Mad plane of the vacancy as reflected in A^2, tends to be much stronger than to the M plane in the case of VV^-.

Another approach could be to follow the suggestion of Sieverts [11], that the electron is localised not just in the mirrorplane, but especially along the chain of atoms pointing from the vacancy in the [011] direction. When plotted against the distances of the atom positions along this chain the tensors Mad1 - Mad6 show a surprisingly good exponential decrease. Moreover also the tensors Mad8 and Mad12 fall on the line if we assume them to belong to the seventh and eight lattice site in this chain as is shown in fig.9. Another argument to choose just Mad8 and Mad12 is that the complete hyperfine data of Mad1 - Mad6, Mad8 and Mad12 are all very similar, in contrast to the other Mad tensors. (These data will be published shortly in a more comprehensive publication). In this picture a wave function emerges which is even more delocalised, though just in one particular direction in space. Parameters of a fit to exponential decrease under this assumpion are also given in table III.

Acknowledgements
The authors wish to thank Drs. R. van Kemp and Dr. E.G. Sieverts for their help in the experiments and analysis, as well as for the many discussions.

REFERENCES

[1] Watkins, G.D.: Radiation Damage in Semiconductors (Paris: Dunod, 1965), 97.
[2] Watkins, G.D., Troxell, J.R. and Chatterjee, A.P., Inst. Phys. Conf. Ser. 46 (1979), 16.
[3] Watkins, G.D., Troxell, J.R., Phys. Rev. Lett. 44 (1980), 593.
[4] Watkins, G.D., Chatterjee, A.P. and Harris, R.D., Inst. Phys. Conf. Ser. 59 (1981), 199 and
Newton, J.L., Chatterjee, A.P., Harris, R.D. and Watkins G.D., this volume.
[5] Bernholc, J., Lipari, N.O., Pantelides, S.T. and Scheffler, M. Inst. Phys. Conf. Ser. 59 (1981), 1.
[6] Baraff, G.A., Kane, E.O. and Schlüter, M., Inst. Phys. Conf. Ser. 59 (1981), 19.
[7] de Wit, J.G., Sieverts, E.G. and Ammerlaan, C.A.J., Phys. Rev. B 14 (1978), 3494.
[8] Sieverts, E.G., Muller, S.H. and Ammerlaan, C.A.J., Phys. Rev. B 18 (1976), 6843.
[9] Watkins, G.D., Inst. Phys. Conf. Ser. 16 (1973), 228.
[10] Watkins, G.D., Inst. Phys. Conf. Ser. 23 (1975), 1.
[11] Sieverts, E.G., J. Phys. C 14 (1981), 2217.